Chemical Engineering Journal 385 (2020) 123950

Contents lists available at ScienceDirect

Chemical Engineering Journal

journal homepage: www.elsevier.com/locate/cej

Investigation of tetracyclines transport in the presence of dissolved organic matters during struvite recovery from swine wastewater

Zhi-Long Ye[a], Jianqiao Zhang[a,b], Jiasheng Cai[a,b], Shaohua Chen[a,*]

[a] Key Laboratory of Urban Pollutant Conversion, Institute of Urban Environment, Chinese Academy of Sciences, No. 1799 Jimei Road, Xiamen City, Fujian 361021, China
[b] University of Chinese Academy of Sciences, Beijing 100049, China

HIGHLIGHT

- Antibiotics exert pollution danger to phosphorous recovery from wastewater.
- DOM existence significantly improves TCs residue in phosphorus recovery.
- Struvite crystals adsorbing DOM-TCs complex contribute significant TCs transport.
- Larger-molecular-weight DOM promotes TCs transport through aggregation.
- The main goal is addressed to control impacts of TCs residue in phosphorus recovery.

ARTICLE INFO

Keywords:
Struvite
Antibiotic
Dissolved organic matter
Adsorption
Phosphorus recovery

ABSTRACT

Struvite ($MgNH_4PO_4{\cdot}6H_2O$) crystallization is preferable for phosphorus recovery from swine wastewater. However, the extensive existence of tetracyclines (TCs) in the wastewater will pose pharmacological threats of recovered products to the environment. In this study, the evolution effects of dissolved organic matters (DOM), as a common media, in the wastewater on TCs migration during struvite recovery from swine wastewater were investigated. Compared to 1.85–7.29 μg/g TCs adsorbed by pure struvite crystals, 148.3–303.9 μg/g TCs were detected in the struvite products recovered under real wastewater. Struvite crystals adsorbing DOM-TCs complex contributed 26.4–30.1% of total TCs migration in the recovery process. A tangential flow filtration system was employed to divide DOM into five fractional parts on the basis of molecular weight cut-offs, i.e. 100 kDa-0.45 μm (FDOM1), 30–100 kDa (FDOM2), 5–30 kDa (FDOM3), 1–5 kDa (FDOM4) and < 1 kDa (FDOM5), respectively. Results revealed that struvite recovery under FDOM1, FDOM2 and FDOM3 with larger molecular weights underwent more organic loss in the aqueous phase due to aggregation and struvite adsorption, and thereafter possessed higher TCs residues in the recovered solids. Due to the electrostatic force, humic acid-like and soluble microbial by-product-like organics were prone to complex with TCs, which promoted TCs transport through the adsorption onto formed struvite crystals. The outcomes were helpful to understand the behaviors of antibiotic migration and develop abatement methods for phosphorus recovery.

1. Introduction

The boom of economic growth and urbanization in the developing countries has generated a large demand on pork production. For instance, there are more than 690 million pigs produced in China annually [1]. Such big animal farming has resulted with numerous discharge of swine wastewater in rich ammonium and phosphorus, which has posed great risks to the environment. Presently, phosphorus recovery from livestock wastewater gained extensive attention worldwide [2,3], since the recovery products can be used as agricultural fertilizers to relieve the global scarcity of phosphorus rock resources [4,5]. Among the methods of phosphate recovery, struvite ($MgNH_4PO_4{\cdot}6H_2O$) crystallization is preferable since it can remove ammonium and phosphate simultaneously, and the recovery product can be utilized as a good fertilizer with the slow-release property [6,7].

Veterinary antibiotics are commonly used as food additives in animal breeding to prevent disease spread and improve the animal feed uptake. According to the literature, about 97,000 tons of antibiotics are used in China annually for pig production [5]. It has been reported that 40–90% antibiotics are not easily digested by the animal gut, and

* Corresponding author.
E-mail address: shchen@iue.ac.cn (S. Chen).

https://doi.org/10.1016/j.cej.2019.123950
Received 22 October 2019; Received in revised form 20 December 2019; Accepted 25 December 2019
Available online 27 December 2019
1385-8947/

subsequently are excreted into the environment [8,9], which exert potent pollution danger to the environment by triggering and spreading the antibiotic resistance genes [10]. Among veterinary antibiotics, tetracyclines (TCs) are widely used in livestock and aquaculture feeding [11]. The extensive TCs existence at ng/L to μg/L levels in treated wastewater, surface water, groundwater has been reported, which poses a threat to the local ecology by promoting the development and spread of antibiotic resistance genes among environmental microorganisms [12,13,14,15]. The transport mechanisms of TCs in the environment include cation exchange, hydrogen bonding formation, electrostatic interaction, electron donor–acceptor and π-π dispersion [16], which can be ascribed to the amphoteric molecules with multiple ionized groups, including tricarbonyl group, phenolic diketone moiety and dimethylamino group [11,17].

According to our previous works conducted under synthetic wastewater [11], struvite crystals could adsorb TCs through electrostatic adherence, and the maximum capacities were CTC 1771.0 μg/Kg, OTC 1494.7 μg/Kg and TC 2094.0 μg/Kg, respectively [11]. For the real livestock wastewater, as a complex and heterogeneous mixture of organic compounds, dissolved organic matters (DOM), do ubiquitously exist with high concentrations. Since DOM possesses various functional groups, TCs can complex with DOM through ion exchange, cation bridging and hydrogen bonding, and thereafter alters TCs solubility, sorption, mobility, bioavailability [18–20]. Subsequently, the environmental risks of TCs will be changed. Investigation on the effects of pH, cations, DOM constituents, including humic substances, polysaccharides and proteins etc., on TCs transport in the environment was also reported by the literature [17,21,22]. However, few works has been reported by now on DOM affecting TCs migration behavior during phosphorus recovery from real wastewater, which will provide helpful information for understanding the impact factors and developing effective methods to control TCs migration.

For struvite precipitation, it should be conducted under alkaline conditions, and the dramatic reduction of ion strength and subsequent formation of struvite crystals in the wastewater will take place. Such variation might change DOM properties and trigger TCs transport from the aqueous phase to the recovered solids. In the present study, the comparison of TCs residues in recovered struvite solids between DOM existence and synthetic wastewater was conducted. The effects of DOM evolution processes and component variation on the discrepancy of antibiotic transport behaviors were examined, and the main DOM constituents contributing to TCs migration were discussed.

2. Materials and methods

2.1. Chemicals and standards

In the present study, three TCs standards, including tetracycline (TC), oxytetracycline (OTC) and chlortetracycline (CTC), with purity above 99.0% were purchased from the Alladin Ltd. US. Their properties were listed in the Supplement Materials. Tetraclycline-D_6 was adopted as the internal standard, and was obtained from the Toronto Research Chemicals Inc. (North York, Canada). For the sample pretreatment, Oasis HLB cartridges (size of 200 mg, 6 mL) were used and obtained from Waters (Milford, USA).

Real swine wastewater was obtained from the digested effluent of a treatment process in an intensive pig farm, located in Xiamen City, China. Filtration by using 0.45 μm pore size of glass fiber filters was firstly conducted to remove suspended organics. After the filtration, the properties of the wastewater were displayed in Table 1. As to TCs, their concentrations were (μg/L): TC 516.3 ± 6.51, OTC 449.3 ± 9.45, CTC 238.7 ± 6.66, respectively.

For struvite precipitation, chemical agents, including $MgCl_2$ and NaOH, were all chemical pure and purchased from Xi Long Co. (China). Ultrapure water was produced by an apparatus of a Milli-Q water purification system, brought from Millipore (Boston, USA).

Table 1
Property of swine wastewater after removing suspended organics.

Item	Concentration (mg/L)	Item	Concentration (mg/L)
pH	7.8 ± 0.1	NH_4^+-N	1662.15 ± 0.11.5
TOC	418.6 ± 10.2	NO_3^--N	68.5 ± 0.5
VSS	82.4 ± 5.5	Total nitrogen	2100.57 ± 21.28
PO_4^{3-}-P	91.57 ± 0.82	SO_4^{2-}	66.8 ± 3.1
Total phosphorus	101.14 ± 1.16		

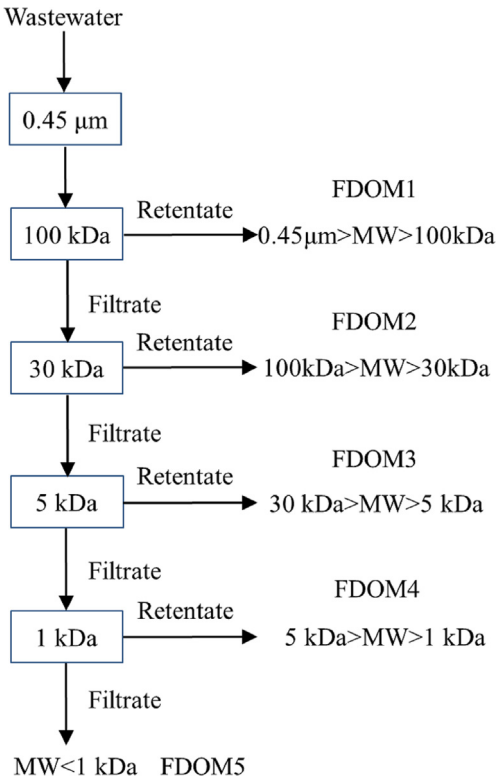

Fig. 1. DOM fractionation by the tangential flow filtration system with different molecular-weight cuts. MW, molecular weight.

2.2. DOM fractionation

Membrane fractionation based on the molecular weight was conducted, and the process was illustrated in Fig. 1. A tangential flow filtration (TFF) system of PALL Minimate (Pall Life Sciences Co., USA) was employed to fractionate DOM into five fractional DOMs (FDOM). A series of membranes (PALL Omega™, US) with different molecular weight cut-offs, i.e. 100 kDa, 30 kDa, 5 kDa and 1 kDa, were selected, by referencing the literature [23]. As shown in Fig. 1, the wastewater filtrate was filtrated sequentially into five fractional DOMs, i.e. 100 kDa-0.45 μm (FDOM1), 30–100 kDa (FDOM2), 5–30 kDa (FDOM3), 1–5 kDa (FDOM4) and < 1 kDa (FDOM5), respectively. To evaluate the fractionation process, the volumes of the retentate and filtrate before and after each fractionation operation were measured, and the DOM recovery (as %DOC) was calculated. %DOC was determined as the total DOC quantities in the retentate and filtrate divided by the total DOC contents in the original wastewater before fractionation.

2.3. Experimental design and setup

In order to screen out the effects of DOM on TCs transport in struvite precipitation, two blank experiments were conducted. The objective of first blank experiment was to investigate TCs adsorption by pure

struvite crystals. Struvite crystallization was carried out by mixing certain amount of stock solutions containing PO_4^{3-}, NH_4^+, Mg^{2+} and TCs, which were prepared by melting $MgCl_2{\cdot}6H_2O$, $(NH_4)_2HPO_4$ and TCs into the ultrapure water, respectively. The ionic concentration levels were referred to Table 1, while TCs were dosed into the liquid with their concentrations similar to the real wastewater. Struvite precipitation was performed by dosing 2 mol/L NaOH to keep pH at 9.3 throughout the experiment, and desired amount of magnesium solution was added into the liquid to control initial Mg:P molar ratio at 1.2:1. After 45 min agitation, the mixture was subjected to solid and liquid separation by centrifugation at 5000 rpm for 20 min. The aqueous and solid samples were separately withdrawn for further analyses.

As to the second blank experiment, its goal was to investigate TCs adsorption by struvite crystals adsorbing DOM. It has been reported that TCs are easily complexing with DOM to form binary complexes (defined as DOM-TCs) [24,25]. Struvite precipitation was conducted in the synthetic solutions by setting the same operational conditions as those in the first blank experiment. The products of struvite crystals were collected by centrifugation, and then were dosed into the real wastewater which contained initial amounts of TCs. After 60 min stirring, the mixture was subjected to solid and liquid separation by centrifugation at 5000 rpm for 20 min. The adsorption capacity of struvite crystal on TCs at the existence of DOM was measured.

Real wastewater containing DOM contents was directly subjected to struvite precipitation by dosing desired Mg^{2+} solution volume and to control Mg:P molar ratio at 1.2:1, and the precipitation was achieved by setting the same conditions as those in the first blank experiment. After that, a series of experiments were carried out to examine the effects of DOM on TCs transport, and the wastewater was filtrated sequentially into five fractional DOMs, as described in Section 2.2. Before struvite reaction, every solution was diluted to keep every FDOM at 150 mg/L. After struvite crystallization, the aqueous and solid samples were respectively withdrawn, and the variations of TOC and TCs in the individual solution were investigated.

2.4. Analytical methods

2.4.1. Common methods

The regular parameters of the wastewater (Table 1), including total nitrogen, total phosphorus, phosphate (PO_4^{3-}-P), volatile suspended solids (VSS) and sulfate, were measured based on the standard methods. Mg ion was determined by inductively coupled plasma optical emission spectroscopy (Optima 7000DV, PerkinElmer, USA). DOC was determined by a TOC analyzer (TOC-Vcph, Shimadzu, Japan). The determination of anionic ions, including nitrate (NO_3^-) and sulfate (SO_4^{2-}), was conducted by using ion chromatograph (Aquion ICS, Thermo Fisher, USA).

The crystalline struvite products were analyzed with X-ray diffraction (XRD, X'Pert PROMPD, Holland). The functional groups of individual FDOMs were assayed by the Fourier transform infrared spectroscopy (FTIR) (iS10, Thermo Fisher Scientific Co., USA) after they were freeze-dried. The analysis of UV–Vis was conducted by using the DR5000 spectrophotometer (Hach, USA), and the data was picked up when the UV absorbance was at λ 254 nm (UV_{254}).

2.4.2. Tetracyclines assay

TCs determination was conducted by using the chromatography/tandem mass spectrometry (LC-MS/MS) (ABI3200 QTRAP, USA) equipped with Phenomennex Kinetex Symmetry C18 column (4.6 mm × 100 mm) for antibiotics identification and quantitation. The mass spectrometry system was installed with electrospray ionization (ESI) source, and was run with the positive mode with desolvation temperature at 300 °C and capillary voltage 5.5 KV. During TCs analyses, recovery rate, detection limits and the quantification for the instrument were determined by using calibration curves, which has been reported in our previous works [11]. Details of the analytical methods was described in the Supplemental Materials.

Table 2
Integral fluorescence region of various DOM components.

Region	Compounds	Emission (nm)	Excitation (nm)
I	Aromatic protein I	280–330	220–250
II	Aromatic protein II	330–380	220–250
III	Fulvic acid-like	380–500	220–250
IV	Soluble microbial by-product-like	280–380	250–280
V	Humic acid-like	380–500	250–400

Before TCs analyses, the pretreatment method of solid-phrase extraction was adopted to extract and concentrate TCs from the samples. Firstly, all the solid and liquid samples were diluted to approximately 200 mL with Milli-Q pure water, and acidified to pH 3.0 by dosing 0.1 mol/L HCl. Oasis HLB cartridge (200 mg/6 mL, Waters, Milliford, USA) was then used to extract TCs from the samples, as described by our previous works [11].

2.4.3. Fluorescence spectrum analyses

In order to analyze the changes of DOM before and after struvite precipitation, three-dimensional excitation and emission matrix fluorescence (3DEEM) spectroscopy was employed by using a fluorescence spectrofluorometer (F-4600, Hitachi Co., Japan) equipped with a 150-W Xenon arc lamp as the light source, and the spectrum was further evaluated by using the method of fluorescence regional integration (FRI) [26]. Generally, 3DEEM was defined into five excitation-emission regions (Table 2) on the basis of the fluorescence of model compounds [26]. The collected data were processed by Origin 8.0 (Origin Lab Inc., USA).

3. Results

3.1. TCs residue in the recovered solids

TCs contents in recovered solids under real or synthetic wastewater were compared. As presented in Fig. 2, 148.3-303.9 μg/g TCs were detected in the recovered struvite solids using real wastewater, significantly higher than those (1.85–7.29 μg/g TCs) in struvite crystals generated in synthetic wastewater. These results suggested that the existence of DOM significantly promoted TCs contents in the recovered products, though DOM aggregation, struvite adsorbing DOM-TCs

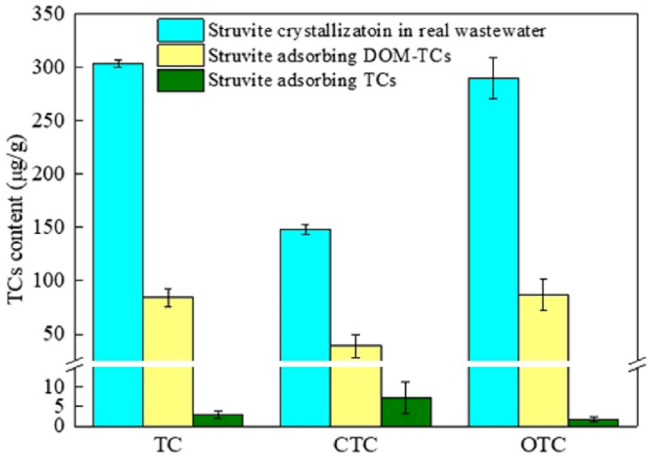

Fig. 2. TCs contents in the struvite products under real and synthetic wastewaters, respectively. Turquoise columns, TCs contents in the recovered solids of struvite recovery from real wastewater; yellow columns, struvite crystals adsorbing DOM-TCs compounds; green columns, pure struvite crystals adsorbing TCs. (For interpretation of the references to colour in this figure legend, the reader is referred to the web version of this article.)

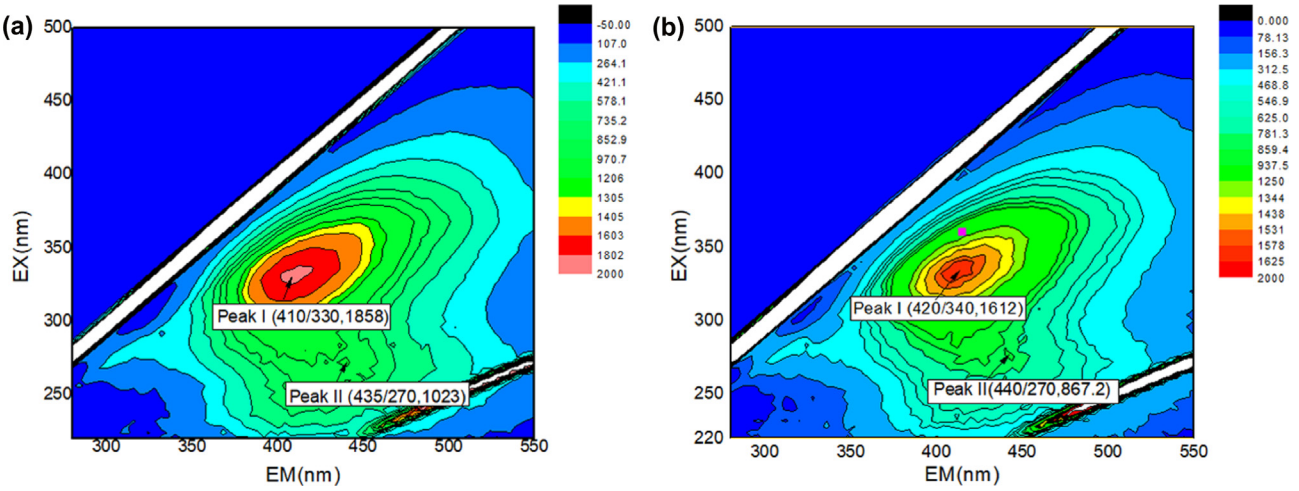

Fig. 3. Fluorescence spectrum of DOM in real wastewater before (A) and after (B) struvite precipitation.

complex and DOM aggregation. Details will be discussed in the latter text.

The fluorescence spectra of the real wastewater before and after struvite crystallization were further investigated. Two main peaks were observed in the samples (Fig. 3) with the emission/excitation wavelengths (Em/Ex) approximate at 410/430 nm (Peak I) and 435/270 nm (Peak II), respectively, which belonged to humic acid-like substances as reported in literature [26,27]. Peak shift and intensity decrease of the fluorescence spectrum were observed after struvite precipitation (Fig. 3). For Peak I, a red-shift (10 nm) along the excitation axis to longer wavelengths and a blue-shift (10 nm) along the emission axis to longer wavelengths were observed, whereas Peak II possessed a red-shift (5 nm) along the emission axis to shorter wavelengths. As described in previous researches, red shift in the fluorescence spectra could be ascribed to the generation or amplification of functional groups, including hydroxyl, carbonyl, alkoxyl, amino and carboxyl constituents [28,29]. As to blue shift, it was regarded as the reduction of condensed aromatic moieties, including the disintegration of π-electron system, number reduction of aromatic rings, disassembling of conjugated bonds in carbon chain structures [29]. It should be noted that the intensity decreases of the fluorescence spectrum were occurred evidently as shown in Fig. 3, where the intensity of Peak I and Peak II were respectively reduced 248.0 and 155.8 after struvite precipitation. Hence, the phenomena of peak reduction and shifts could be ascribed to DOM co-precipitation with struvite or partly hydrolysis, which was also verified by the variation of TOC and UV_{254} values in Table 3. These results indicated that during struvite crystallization DOM evolution, including concentration reduction and component variation, significantly promoted TCs transport.

Besides, from Fig. 2, it should be noted that struvite crystals adsorbed 39.1–87.4 μg/g DOM-TCs complex, which occupied 26.4–30.1% TCs removal from the wastewater. A matching reduction of TOC in wastewater from 418.6 mg/L to 376.7 mg/L, coupling with UV_{254} decrease from 0.356 to 0.339 was observed in Table 3. This result indicated that if we want to exam the TCs transport behavior during phosphate recovery from wastewater, the adsorption of DOM-TCs complex by struvite crystals should not be ignored. Furthermore, as presented at the bottom line of Table 3, more DOM loss in the aqueous phrase after struvite precipitation was observed, with the concentrations decrease from 418.6 mg/L to 309.7 mg/L. Such DOM deduction suggested that in addition to DOM adsorption by struvite crystals, significant parts of DOM destabilized and co-precipitated with struvite precipitation, which consequently promoted TCs transport from the liquid phase to the solids.

Table 3
TOC and UV_{254} of the liquid before and after struvite precipitation.

Type	TOC (mg/L)	UV_{254}
Raw wastewater	418.6 ± 3.4	0.356 ± 0.12
Supernate after struvite crystal adsorption	376.7 ± 6.0	0.339 ± 0.05
Supernate after struvite precipitation	309.7 ± 4.1	0.271 ± 0.144

3.2. TCs residues in fractionated DOMs

In order to investigate the changes of DOM components and their effects on TCs transport behaviors, a tangential flow filtration (TFF) system was adopted to fractionate DOM into five fractional DOMs (FDOMs), which was based on the molecular weight cut-offs, i.e. 100 kDa-0.45 μm (FDOM1), 30–100 kDa (FDOM2), 5–30 kDa (FDOM3), 1–5 kDa (FDOM4) and < 1 kDa (FDOM5), respectively. They were further subjected to struvite precipitation. As displayed in Fig. 4A, FDOMs with larger molecular weights displayed much higher capability on TCs transport in struvite recovery. TCs residues in the recovered solids were detected at 250.8–733.7 μg/g, 131.5–482.0 μg/g, 137.1–199.4 μg/g, 51.3–52.9 μg/g and 36.2–225.3 μg/g for FDOM1, FDOM2, FDOM3, FDOM4 and FDOM5, respectively. Meanwhile, these FDOMs with larger molecular weighs underwent more organic loss in the aqueous phase, and consequently transferred much more to the recovered products as shown in Fig. 4B.

As described in Section 3.1, peak shifts and intensity reduction of the fluorescence spectra during struvite recovery could be used to indicate DOM's destabilization and co-precipitation with struvite particles, adsorption by struvite crystals and partly hydrolysis, which might consequently promote TCs transport behavior. The analyses on the fluorescence spectra of different FDOMs were conducted. Discrepancies of peak shifts and intensity changes before and after struvite precipitation were illustrated in Fig. 5. According to the peak locations of fluorescence spectra (Table 4), Peak A and B with higher intensities were defined as humic acid-like and aromatic protein II materials, where Peak C with lower intensity was preferred as soluble microbial by-product-like organics. As for Peak A, the intensities of all FDOMs (FDOM5 undetected) possessed distinct changes, while most of the emission/excitation wavelengths (Em/Ex) after struvite precipitation moved to smaller values along the emission/excitation axes. These peak shifts to smaller wavelengths were not defined to red-shift or blue shift [28,29], which indicated that humic acid-like organics might aggregate or adsorb onto struvite particles, and did not disintegrate in struvite precipitation. With regard to Peak B, blue-shifts coupling with clear intensity reductions were detected in all FDOMs with the emission

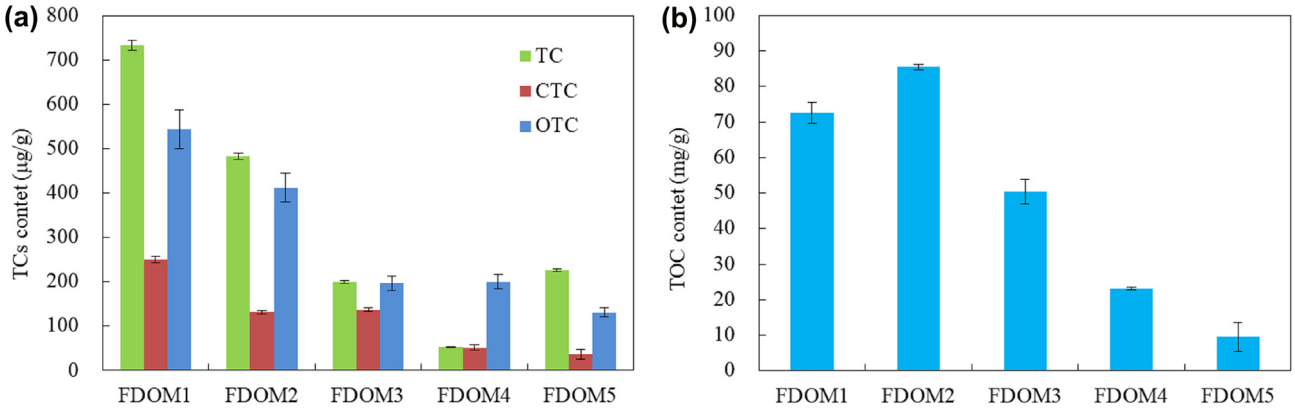

Fig. 4. TCs (A) and TOC (B) contents in the recovered solids under different fractional DOMs as the media. FDOM1, 100 kDa-0.45 μm; FDOM2, 30–100 kDa; FDOM3, 5–30 kDa; FDOM4, 1–5 kDa; FDOM5, < 1 kDa.

wavelengths moved to larger values after struvite precipitation, which revealed that the aggregation and hydrolysis of aromatic protein organics in the wastewater were taken place simultaneously. Regarding Peak C, moderate intensity changes were observed after struvite crystallization. Considering that none red-shift or blue shift was occurred in all FDOMs (Table 3), the adsorption of soluble microbial by-product-like materials by struvite crystals was expected predominantly.

The fluorescence regional integration (FRI) method [26] was employed to analyze the differences organic components of FDOMs before and after struvite precipitation. As displayed in Fig. 6, struvite crystallization resulted with much more DOC loss in FDOMs with higher molecular weights. 45.6% FDOM1, 41.0% FDOM2, 21.8% FDOM3, 16.1% FDOM4 and 10.3% FDOM4 were removed from the aqueous phase, respectively. These results echoed that much more TCs transport occurred in FDOMs with higher molecular weight cut-offs, as presented in Fig. 4. Regarding the DOM components, humic acid-like (Region V), soluble microbial by-product-like (Region IV) and fulvic acid-like (Region III) organics in the FDOMs with higher molecular weights, such as FDOM1, FDOM2 and FDOM3, displayed distinct reduction from the wastewater, which could be ascribed to the aggregation and co-precipitation with struvite particles and adsorption by struvite crystals, as described in the above text. For the FDOMs with smaller molecular weights, i.e. FDOM4 and FDOM5, humic acid-like (Region V), soluble microbial by-product-like (Region IV) and fulvic acid-like (Region III) materials had less occupation, and illustrated less loss after struvite precipitation (Fig. 6). As to proteins, aromatic protein I (Region I) possessed a slight increase after struvite precipitation, while the concentrations of aromatic protein II (Region II) in FDOMs displayed obvious decrease. These results confirmed that the phenomena of removal and disintegration of aromatic protein organics in the wastewater were taken place simultaneously during the struvite precipitation, which has been described in the above text.

4. Discussion

Phosphorus recovery from livestock wastewater as struvite has gained extensive attention today and has been applied widely [2,30,31]. Our previous studies revealed that struvite recovery from wastewater promoted obvious antibiotics transport from the liquid phase to the recovered products, which consequently posed potential ecological risks to the environment [5,32]. As shown in Fig. 2, the existence of DOM in real wastewater resulted in 148.3–303.9 μg/g TCs detected in the recovered products, significantly higher than 1.85–7.29 μg/g TCs in struvite crystals generated in synthetic wastewater. In addition, Fig. 2 also illustrated that struvite crystals adsorbing DOM-TCs complex should be considered, since it contributed 26.4–30.1% total TCs transport in the recovery process. Therefore, it is crucial to clarify the variation of DOM and the components for understanding TCs migration in the process of struvite recovery from wastewater.

For the chemical struvite reaction, the pH values of wastewater would be enhanced to alkaline conditions, and the solid struvite crystals would be formed coupling with a dramatic reduction of ion strength in the wastewater. As a result, such significant variation of wastewater properties would make DOM undergo several processes, including: (1) altering the surface charge characteristics of DOM; (2) reducing repulsive interactions among negatively charged molecules of DOM [33,34] and subsequently leading to aggregation among certain parts of DOM constituents [35]; (3) adsorbing by the formed struvite particles since the surface of crystallites are positively charged [36]; (4) being in favor of small parts of DOM hydrolyzing under the alkaline circumstances [32,37]. It should be noted that DOM is a heterogeneous mixture of organic compounds and contains complex functional groups. During struvite recovery, the four DOM evolution processes occurred simultaneously, which was indicative that it was difficult and complicated to quantify the effects of DOM evolution processes and component variation on the discrepancy of antibiotic transport behaviors.

In the present study, DOM was filtrated sequentially into five fractional DOMs, and all the FDOMs were subjected to the FTIR spectra analyses (Fig. 7). The features of these characteristic spectra and relevant assignments have been described by other literatures [22,37–40]: (a) two sharp bands at 700 and 835 cm^{-1} belongs to the N\H vibration of primary amine group and secondary amine group respectively; (b) small peaks at 1274 and 1399 cm^{-1} are assigned to aromatic –COOH peak and phenolic hydroxyl stretching vibrations, respectively; (c) the bands at 1460–1420 cm^{-1} are attributed to C–H deformation of aliphatic and CH_3 groups, respectively; (d) the absorption at about 1645 cm^{-1} is assigned to the C\O stretching of secondary alcohols and/or ethers; (e) sharp bands at 2300–2400 cm^{-1} are attributed to the deformation of phenolic hydroxyl; (f) a series shoulders at about 2920, and 3437 cm^{-1} can be assigned to symmetric and asymmetric stretching of aliphatic methyl and methylene groups, such as fatty acids and various aliphatic. According to previous claims [23,41], DOM with higher molecular weights had higher aromaticity with more functional groups, such as acidic moieties, polysaccharides, fatty acids and long aliphatic side chains, and therefore could chelate with TCs more easily. As a result, struvite recovery under FDOM1, FDOM2 and FDOM3 with larger molecular weight underwent more organic loss through aggregation and struvite adsorption in the aqueous phase, which was also supported by the variation of FDOM components, including humic acid-like, soluble microbial by-product-like and fulvic acid-like organics (Fig. 6). Hence, FDOMs with higher molecular weights possessed higher TCs residues in the recovered solids, as shown in Fig. 4.

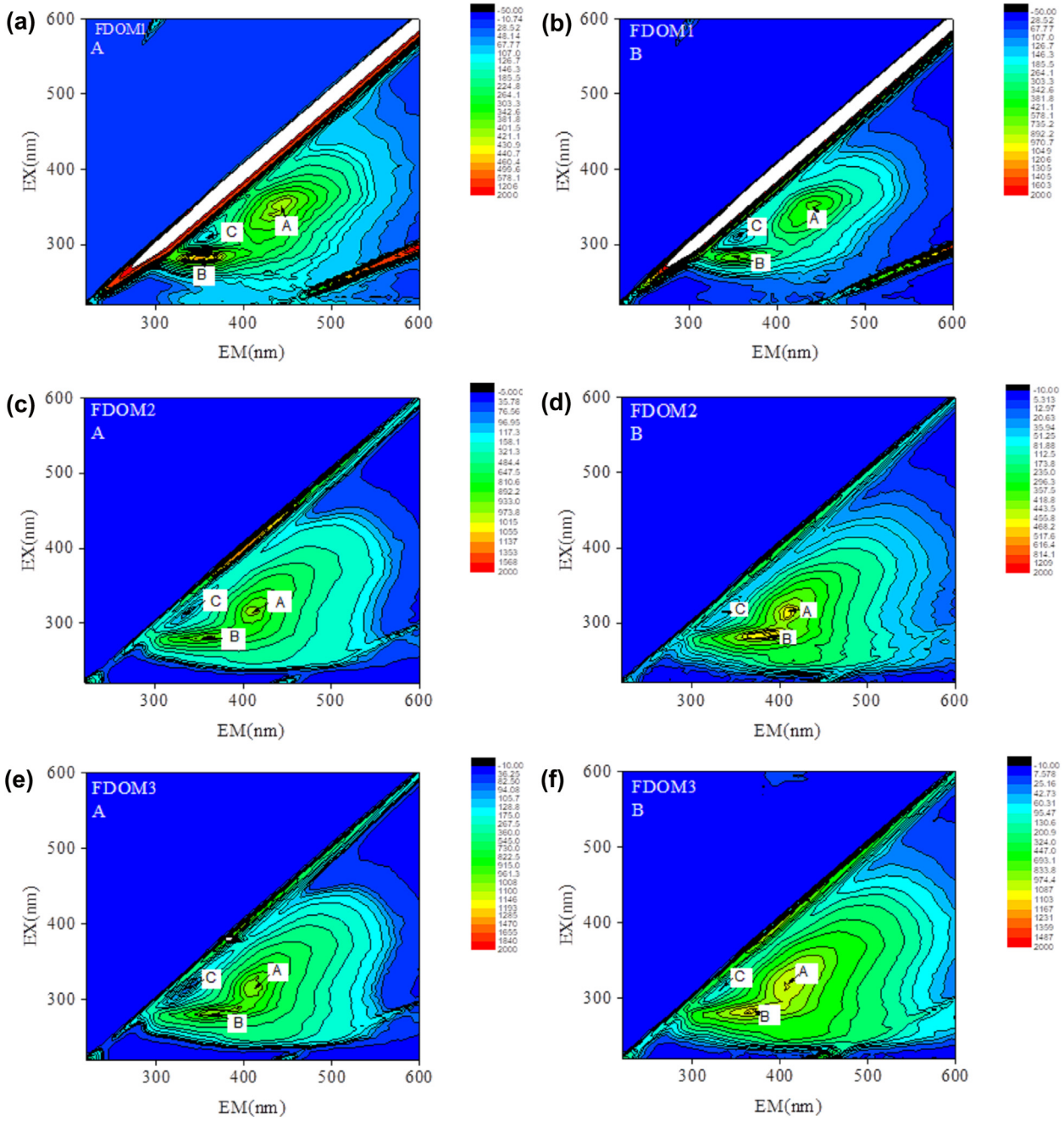

Fig. 5. Fluorescence spectrum of fractional DOMs before (A) and after (B) struvite precipitation. FDOM1, 100 kDa-0.45 μm; FDOM2, 30–100 kDa; FDOM3, 5–30 kDa; FDOM4, 1–5 kDa; FDOM5, < 1 kDa.

It should be noted that 26.4–30.1% TCs residues in the recovered products contributed to DOM complexation (DOM-TCs) and subsequent adsorption by struvite crystals (Fig. 2). In order to clarify the functional DOM components, the analyses on peak shifts and intensity discrepancy of FDOMs fluorescence spectrum were conducted. As described in RESULT section, the occurrence of fluorescence peak intensity discrepancies suggested that DOM components were subjected to concentration variation. Under the preconditions of intensity changes, red shift or blue shift of the fluorescence peaks could be ascribed to the generation of functional groups or the reduction of condensed aromatic moieties [28–30], which indicated that parts of DOM components were disintegrated or hydrolyzed during struvite precipitation. Contrarily, fluorescence peaks non-shifting or moving to the lower wavelengths along the excitation/emission axis implied that none of new compounds were generated, and therefore intensity variation could be attributed to DOM components partly adsorbing by the struvite crystals. Results (Fig. 5 and Table 4) revealed that the reduction of humic acid-like and soluble microbial by-product-like organics was partly ascribed to the adsorption by formed struvite crystals, while aromatic protein organics in portion possessed simultaneously aggregate and hydrolyze. It should be pointed out that different from the interaction mechanisms of ion exchange, cation bridging and H-bonding under acidic and neutral conditions [17,33], the predominant chelation mechanism of humic acid-like or soluble microbial by-product-like organics interacting with TCs under alkaline circumstance was electrostatic force [15,23,38,42]. This was because under alkaline conditions the functional moieties of carboxylic and phenolic groups in humic acids and soluble microbial by-product-like materials were deprotonated [17,25], and TCs did exist with the phenolic diketone moiety negatively charged [11]. Hence, the affinity of TCs with humic acids or soluble microbial by-product-like

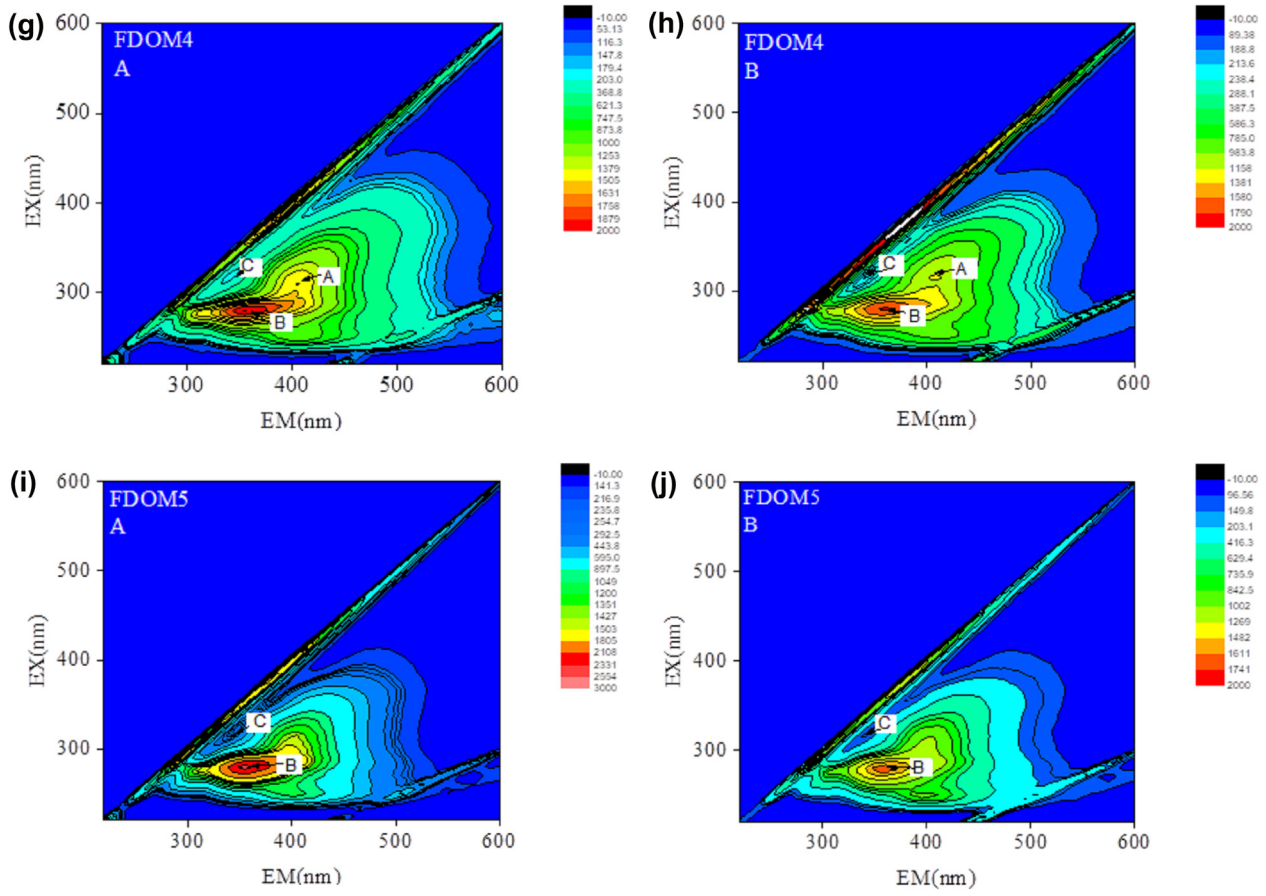

Fig. 5. (*continued*)

materials was dominant by the electrostatic force. Meanwhile, due to the crystallite facets were rich in $Mg[H_2O]_6^{2+}$ with positive charges [11], struvite crystals were prone to adsorb negatively charged DOM-TCs complex. Consequently, 39.1–87.4 μg/g DOM-TCs complex adsorbed by the struvite crystals were detected as illustrated in Fig. 2. This clarification was helpful for understanding TCs transport in the process of struvite recovery from wastewater.

5. Conclusion

This study was conducted to screen out the effects of DOM components on TCs transport during struvite recovery from wastewater. Compared to 1.85–7.29 μg/g TCs adsorbing by pure struvite crystals, 148.3–303.9 μg/g TCs were detected in the struvite products recovered under real wastewater, which suggested that DOM existence significantly improved TCs residue in the recovered products and might consequently posed potential ecological risks to the environment. It should be pointed out that struvite crystals adsorbing DOM-TCs complex contributed 26.4–30.1% total TCs transport in the recovery process. A tangential flow filtration (TFF) system was employed to divide DOM into five fractional parts on the basis of molecular weight cut-offs, so as to evaluate DOM evolution processes and component variation on the discrepancy of antibiotic transport behaviors. Results revealed that struvite recovery under FDOM1, FDOM2 and FDOM3 with larger molecular weights underwent more organic loss in the aqueous phase through aggregation and struvite adsorption, and thereafter possessed higher TCs residues in the recovered solids. Due to the electrostatic force, humic acid-like and soluble microbial by-product-like organics

Table 4
Sites and intensities of peaks in the fluorescence spectrum of different FDOMs before and after struvite precipitation.

Term	Event	Peak A*		Peak B		Peak C	
		Site (Em/Ex)**	Intensity	Site (Em/Ex)	Intensity	Site (Em/Ex)	Intensity
FDOM1	Before	445/355	420.9	345/280	478.1	350/315	150.5
	After	440/355	435.5	355/285	455.4	345/310	159.6
FDOM2	Before	410/315	960.7	360/290	899	330/315	117
	After	410/340	443.5	390/290	468.2	330/315	81.88
FDOM3	Before	410/315	915	370/290	932	330/320	105.7
	After	405/310	1087	375/285	1082	330/310	130.6
FDOM4	Before	405/305	1379	380/285	2000	335/310	203
	After	405/305	983.8	375/285	1790	330/310	188.6
FDOM5	Before	–	–	360/280	2554	330/310	292.5
	After	–	–	365/280	1611	330/310	96.5

*According to their locations, Peak A, B and C were preferred as humic acid-like, aromatic protein II and soluble microbial by-product-like materials, respectively.
**Em/Ex, the emission/excitation wavelengths.

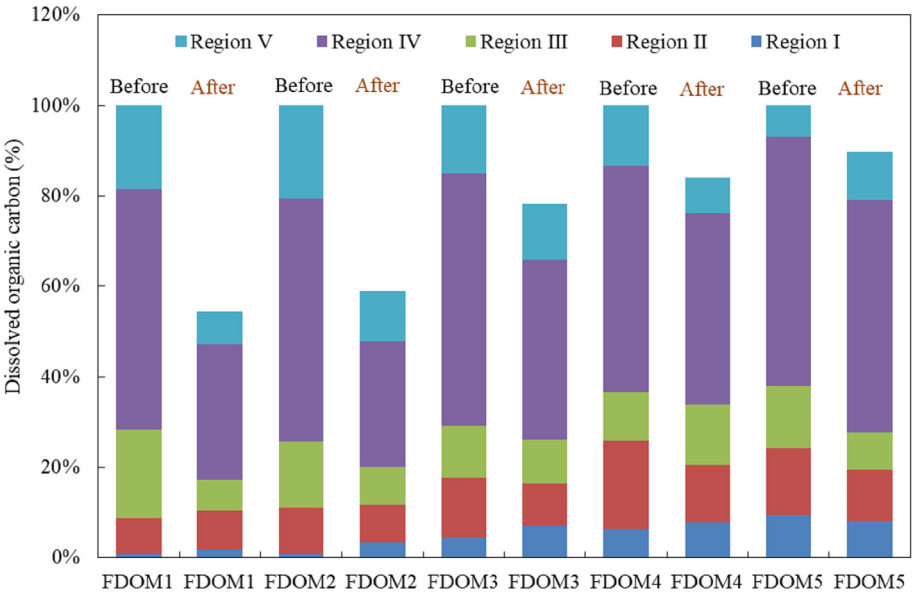

Fig. 6. Dissolved organic constituents in the aqueous phase before and after struvite precipitation. FDOM1, 100 kDa-0.45 μm; FDOM2, 30–100 kDa; FDOM3, 5–30 kDa; FDOM4, 1–5 kDa; FDOM5, < 1 kDa. Region I, aromatic protein I; Region II, aromatic protein II; Region III, fulvic acid-like; Region IV, soluble microbial by-product-like; Region V, humic acid-like.

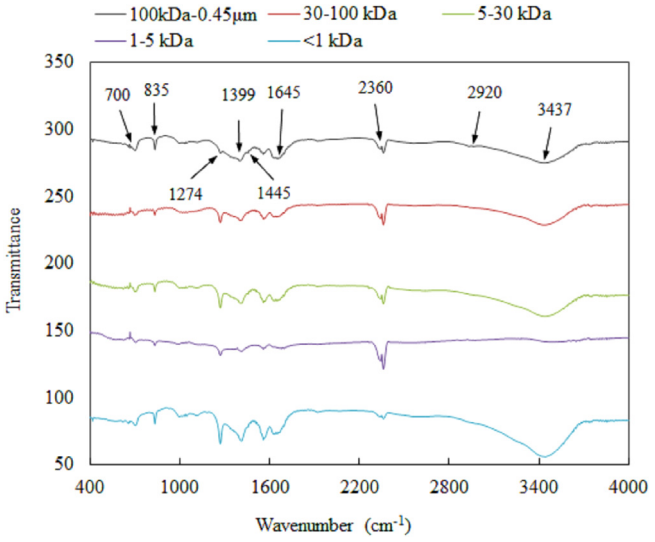

Fig. 7. FTIR spectra of different fractional DOMs with different molecular-weight cut-offs.

were prone to complex with TCs, which promoted TCs transport through the adsorption onto formed struvite crystals. These conclusive outcomes are helpful to understand the behaviors of antibiotic transport during phosphorus recovery from wastewater, and will undoubtedly provide useful information for developing methods to control the pharmacological impacts in the future. In order to control TCs migration during phosphorus recovery, pretreatment method, such as coagulation, is recommended to remove dissolved organics with larger molecular weights. Furthermore, ozonation and ion exchange resin are suggested to degrade or remove DOM-TCs compounds, which can significantly reduce TCs residue in the wastewater and interdict TCs transport to the products of phosphorus recovery.

Declaration of Competing Interest

The authors declare that they have no known competing financial interests or personal relationships that could have appeared to influence the work reported in this paper.

Acknowledgement

This work was supported by the General Project of National Natural Science Foundation of China (No. 51878639).

Appendix A. Supplementary data

Supplementary data to this article can be found online at https://doi.org/10.1016/j.cej.2019.123950.

References

[1] National Bureau of Statistics of the People's Republic of China (NBSPRC), The China Statistical Yearbook 2018. http://www.stats.gov.cn/tjsj/ndsj/2018/indexch.htm, 2018.
[2] S. Piveteau, S. Picard, P. Dabert, M.L. Daumer, Dissolution of particulate phosphorus in pig slurry through biological acidification: A critical step for maximum phosphorus recovery as struvite, Water Res. 124 (2017) 693–701.
[3] L. Wei, T. Hong, X. Li, M. Li, Q. Zhang, T. Chen, New insights into the adsorption behavior and mechanism of alginic acid onto struvite crystals, Chem. Eng. J. 358 (2019) 1074–1082.
[4] Y. Lei, I. Hidayat, M. Saakes, R. van der Weijden, C.J.N. Buisman, Fate of calcium, magnesium and inorganic carbon in electrochemical phosphorus recovery from domestic wastewater, Chem. Eng. J. 362 (2019) 453–459.
[5] Y. Lou, Z. Ye, S. Chen, X. Ye, Y. Deng, J. Zhang, Sorption behavior of tetracyclines on suspended organic matters originating from swine wastewater, J. Environ. Sci. 65 (2017) 144–152.
[6] X.N. Liu, J. Wang, Impact of calcium on struvite crystallization in the wastewater and its competition with magnesium, Chem. Eng. J. 378 (2019), https://doi.org/10.1016/j.cej.2019.122121.
[7] S.E. Mousavi, M.R. Choudhury, M.S. Rahaman, 3-D CFD-PBM coupled modeling and experimental investigation of struvite precipitation in a batch stirred reactor, Chem. Eng. J. 361 (2019) 690–702.
[8] J. Pei, H. Yao, H. Wang, J. Ren, X. Yu, Comparison of ozone and thermal hydrolysis combined with anaerobic digestion for municipal and pharmaceutical waste sludge with tetracycline resistance genes, Water Res. 99 (2016) 122–128.
[9] O.A. Alsager, M.N. Alnajrani, O. Alhazzaa, Decomposition of antibiotics by gamma irradiation: Kinetics, antimicrobial activity, and real application in food matrices, Chem. Eng. J. 338 (2018) 548–556.
[10] Y.G. Zhu, T.A. Johnson, J.Q. Su, M. Qiao, G.X. Guo, R.D. Stedtfeld, S.A. Hashsham, J.M. Tiedje, Diverse and abundant antibiotic resistance genes in Chinese swine farms, Proc. Natl. Acad. Sci. U.S.A 110 (2013) 3435–3440.
[11] Z. Ye, Y. Deng, Y. Lou, X. Ye, J. Zhang, S. Chen, Adsorption behavior of tetracyclines by struvite particles in the process of phosphorus recovery from synthetic swine wastewater, Chem. Eng. J. 313 (2017) 1633–1638.
[12] S. Li, J.Y. Hu, Photolytic and photocatalytic degradation of tetracycline: Effect of humic acid on degradation kinetics and mechanisms, J. Hazard. Mater. 318 (2016) 134–144.
[13] M. Topal, E.I.A. Topal, Occurrence and fate of tetracycline and degradation products in municipal biological wastewater treatment plant and transport of them in surface water, Environ. Monit. Assess. 187 (2015) 750–758.
[14] W.F. Yan, Y. Xiao, W.D. Yan, R. Ding, S.H. Wang, F. Zhao, The effect of

bioelectrochemical systems on antibiotics removal and antibiotic resistance genes: A review, Chem. Eng. J. 358 (2019) 1421–1437.
[15] W.C. Yu, S.H. Zhang, Z.Q. Shen, Q.X. Zhou, D. Yang, Efficient removal mechanism for antibiotic resistance genes from aquatic environments by graphene oxide nanosheet, Chem. Eng. J. 313 (2019) 836–846.
[16] A.C. Martins, O. Pezoti, A.L. Cazetta, K.C. Bedin, D.A.S. Yamazaki, G.F.G. Bandoch, T. Asefa, J.V. Visentainer, V.C. Almeida, Removal of tetracycline by NaOH-activated carbon produced from macadamia nut shells: Kinetic and equilibrium studies, Chem. Eng. J. 260 (2015) 291–299.
[17] I. Christl, M. Ruiz, J.R. Schmidt, J.A. Pedersen, Clarithromycin and tetracycline binding to soil humic acid in the absence and presence of calcium, Environ. Sci. Technol. 50 (2016) 9933–9942.
[18] N. Leminh, S.J. Khan, J.E. Drewes, R.M. Stuetz, Fate of antibiotics during municipal water recycling treatment processes, Water Res. 44 (2010) 4295–4323.
[19] H. Sun, X. Shi, J. Mao, D. Zhu, Tetracycline sorption to coal and soil humic acids: An examination of humic structural heterogeneity, Environ. Toxicol. Chem. 29 (2010) 1934–1942.
[20] L. Li, Z. Li, M. Liu, M. Wu, X. Ma, X. Tang, Structural analysis of organic matter composition in piggery wastewater during the process of organic degradation based on FTIR spectroscopy, Spectrosc. Spectr. Anal. 36 (2016) 3517–3522.
[21] Y. Zhao, J. Geng, X. Wang, X. Gu, S. Gao, Tetracycline adsorption on kaolinite: pH, metal cations and humic acid effects, Ecotoxicology 20 (2011) 1141–1147.
[22] L. Bai, Z. Zhao, C. Wang, C. Wang, X. Liu, H. Jiang, Multi-spectroscopic investigation on the complexation of tetracycline with dissolved organic matter derived from algae and macrophyte, Chemosphere 187 (2017) 421–429.
[23] D. Ma, B. Gao, S. Sun, Y. Wang, Q. Yue, Q. Li, Effects of dissolved organic matter size fractions on trihalomethanes formation in MBR effluents during chlorine disinfection, Bioresour. Technol. 136 (2013) 535–541.
[24] J.R.V. Pils, D.A. Laird, Sorption of tetracycline and chlortetracycline on K- and Ca-saturated soil clays, humic substances, and clay-humic complexes, Environ. Sci. Tech. 41 (2007) 1928–1933.
[25] Y. Ding, B.J. Teppen, S.A. Boyd, H. Li, Measurement of associations of pharmaceuticals with dissolved humic substances using solid phase extraction, Chemosphere 91 (2013) 314–319.
[26] J.A. Korak, E.C. Wert, F. Rosario-Ortiz, Evaluating fluorescence spectroscopy as a tool to characterize cyanobacteria intracellular organic matter upon simulated release and oxidation in natural water, Water Res. 68 (2015) 432–443.
[27] X. Li, M. Xing, J. Yang, L. Zhao, X. Dai, Organic matter humification in vermifiltration process for domestic sewage sludge treatment by excitation–emission matrix fluorescence and Fourier transform infrared spectroscopy, J. Hazard. Mater. 261 (2013) 491–499.
[28] J.R. Helms, A. Stubbins, E.M. Perdue, N.W. Green, H. Chen, K. Mopper, Photochemical bleaching of oceanic dissolved organic matter and its effect on absorption spectral slope and fluorescence, Mar. Chem. 155 (2013) 81–91.
[29] E.E. Lavonen, D.N. Kothawada, L.J. Tranvik, M. Gonsior, P. Schmitt-Kopplin, S.J. Köhler, Tracking changes in the optical properties and molecular composition of dissolved organic matter during drinking water production, Water Res. 85 (2015) 286–294.
[30] Z. Zhang, L. She, J. Zhang, Z. Wang, P. Xiang, S. Xia, Electrochemical acidolysis of magnesite to induce struvite crystallization for recovering phosphorus from aqueous solution, Chemosphere 226 (2019) 307–315.
[31] B. Elduayen-Echave, I. Lizarralde, E. Ayesa, R. Grau, A new mass-based discretized population balance model for precipitation processes: Application to struvite precipitation, Water Res. 155 (2019) 26–41.
[32] Q. Chen, X. An, Y. Zhu, J. Su, M. Gillings, Z. Ye, L. Cui, Application of Struvite alters the antibiotic resistome in soil, rhizosphere, and phyllosphere, Environ. Sci. Technol. 51 (2017) 8149–8157.
[33] C. Gu, K. Karthikeyan, S.D. Sibley, J.A. Pedersen, Complexation of the antibiotic tetracycline with humic acid, Chemosphere 66 (2007) 1494–1501.
[34] N. Carmosini, L.S. Lee, Ciprofloxacin sorption by dissolved organic carbon from reference and bio-waste materials, Chemosphere 77 (2009) 813–820.
[35] M. Baalousha, M. Motelica-Heino, P. Le Coustumer, Conformation and size of humic substances: Effects of major cation concentration and type, pH, salinity, and residence time, Colloid Surf. A-Physicochem. Eng. Asp 272 (2006) 48–55.
[36] J. Prywer, A. Torzewska, Bacterially induced struvite growth from synthetic urine: Experimental and theoretical characterization of crystal morphology, Cryst. Growth Des. 9 (2009) 3538–3543.
[37] D. Li, Y. Zhou, Y. Tan, S. Pathak, M.B.A. Majid, Alkali-solubilized organic matter from sludge and its degradability in the anaerobic process, Bioresour. Technol. 200 (2016) 579–586.
[38] X. Guo, X. He, H. Zhang, Y. Deng, L. Chen, J. Jiang, Characterization of dissolved organic matter extracted from fermentation effluent of swine manure slurry using spectroscopic techniques and parallel factor analysis (PARAFAC), Microchem. J. 102 (2012) 115–122.
[39] E.P. Ng, S. Mintova, Quantitative moisture measurements in lubricating oils by FTIR spectroscopy combined with solvent extraction approach, Microchem. J. 98 (2011) 177–185.
[40] C. Song, X.F. Sun, S.F. Xing, P.F. Xia, Y.J. Shi, S.G. Wang, Characterization of the interactions between tetracycline antibiotics and microbial extracellular polymeric substances with spectroscopic approaches, Environ. Sci. Pollut. Res. 21 (2014) 1786–1795.
[41] P. Kulshrestha, R.F. Giese, D.S. Aga, Investigating the molecular interactions of oxytetracycline in clay and organic matter: insights on factors affecting its mobility in soil, Environ. Sci. Technol. 38 (2004) 4097–4105.
[42] G. Hou, X. Hao, R. Zhang, J. Wang, R. Liu, C. Liu, Tetracycline removal and effect on the formation and degradation of extracellular polymeric substances and volatile fatty acids in the process of hydrogen fermentation, Bioresour. Technol. 212 (2016) 20–25.